Inorg. Chem. **1993,** *32,* 4450–4456

Notes

Metal Ion-Induced Self-Assembly of Functionalized 2,6-Oligopyridines. 4. Metal–Metal Interaction in Double-Stranded, Dicuprous Helicates Derived from Terpyridine Derivatives[1]

Kevin T. Potts,[*,†] Majid Keshavarz-K,[†] Fook S. Tham,[†] Héctor D. Abruña,[*,‡] and Claudia Arana[‡]

Departments of Chemistry, Rensselaer Polytechnic Institute,
Troy, New York 12180, and Cornell University,
Ithaca, New York 14853

Received June 11, 1993

Introduction

Spontaneous generation of functionalized higher order structures is of current interest in modern synthetic chemistry,[2] and in earlier publications[3,4] the self-assembly concepts have been applied to form helical complexes from oligopyridines and transition metals. A number of transition metal complexes obtained from bipyridine and terpyridine have shown a variety of interesting electrochemical[5] and photochemical[6] properties. Bis(vinylbipyridine) and bis(vinylterpyridine) transition metal complexes have been incorporated into constrained environments on polymer-modified electrodes[7a,b] with interesting and useful results. In the terpyridine case the resulting electrode was electrocatalytic for the reduction of carbon dioxide to formate and also for the reduction of oxygen to water and hydrogen peroxide.[7b]

We have been conducting a systematic study[3b,8] of metal–metal interactions and intramolecular electron transfer[9] in a series of multimetallic double-stranded helicates derived from oligopyridines and transition metals. Our choice of these helical systems derives from the ability of the self-assembly process to spontaneously position the metals in close proximity to one another resulting in a series of excellent models of established geometry and structure. Cu(I) complexes which may be obtained in a variety of coordination geometries are of particular interest. In complexes derived from even numbered oligopyridines[3b,8a] the coordination geometry at each metal center was tetrahedral-like, analogous to that of a bis(bipyridine)copper(I) $[\mathrm{L_2Cu^I}]^+$ complex.[10] Complexes derived from odd-numbered oligopyridines present a different situation. Cu(I) complexes of 2-substituted pyridines formed[11] trigonal complexes $[\mathrm{L_3Cu^I}]^+$. Terpyridine, the next odd-numbered ligand, has been proposed to form $[\mathrm{LCu^I}]^+$, $[\mathrm{LCu^I}]_2^{2+}$, or $[\mathrm{L_2Cu^I}]^+$ complexes as well as polymeric systems.[12] However, the evidence presented in the published reports on these terpyridine complexes is not sufficiently definitive to substantiate unambiguously any structural assignments. We believe that these conflicting and irreconcilable reports are, in part, due to the lability and air-sensitivity of terpyridine–Cu(I) complexes, which in solution oxidize readily to give well-known octahedral bis(terpyridine)copper(II) complexes.[13]

We have reinvestigated terpyridine–Cu(I) chemistry. This article reports a novel approach to the stabilization of terpyridine–Cu(I) complexes which should also be readily applicable to other odd-numbered oligopyridines and related heterocyclic ligands. This approach results from the earlier observations[3b,8] that, in several oligopyridine double-stranded helical complexes, appreciable π–π interaction was present between the pyridine rings in adjacent ligand strands. Terpyridine is the simplest oligopyridine capable of forming a double-stranded helicate, and none have been reported to date. Molecular models (CPK) suggested that in a terpyridine–Cu(I) double-stranded helical complex, the overall π–π interaction in the complex would be enhanced by the introduction of 6,6″-phenyl substituents into terpyridine. These substituents, due to their positions in the double-stranded helicate, would also provide the metal centers with a degree of steric protection from the environment.

Experimental Section

Electrochemical and spectroscopic characterizations were performed under the same conditions and using the same intrumentation as reported in a previous publication.[3b]

Synthesis of 6,6″-Diphenyl-4,4″-bis(methylthio)-2,2′:6′,2″-terpyridine (3b). Acetophenone (1.04 g, 8.6×10^{-3} mol), anhydrous THF (25 mL), and potassium *tert*-butoxide (2.12 g, 1.89×10^{-2} mol) were mixed in a previously flame-dried 250-mL round-bottom flask under a N_2 atmosphere, and the resulting yellow suspension was stirred at room temperature for 10 min. 2,6-Bis[3,3-bis(methylthio)-1-oxo-2-propen-1-yl]pyridine[14] (**1a**) (1.60 g, 4.3×10^{-3} mol) in THF (25 mL) was then added dropwise over a 30-min period. The resultant red-colored heterogeneous reaction

---

[†] Rensselaer Polytechnic Institute.

[‡] Cornell University.

(1) Abstracted from the Ph.D. dissertations of M.K. (RPI) and C.A. (Cornell), 1992.

(2) (a) Whitesides, G. M.; Mathias, J. P.; Seto, C. T. *Science* **1991**, *254*, 1312. (b) Lehn, J.-M. *Angew. Chem., Int. Ed. Engl.* **1990**, *29*, 1304.

(3) (a) Gheysen, K. A.; Potts, K. T.; Hurrell, H. C.; Abruña, H. D. *Inorg. Chem.* **1990**, *29*, 1589. Potts, K. T. *Bull. Soc. Chim. Belg.* **1990**, *99*, 741. (b) Potts, K. T.; Keshavarz-K, M.; Tham, F. S.; Abruña, H. D.; Arana, C. *Inorg. Chem.*, two preceding papers in this issue.

(4) (a) Pfeil, A.; Lehn, J.-M. *J. Chem. Soc., Chem. Commun.* **1992**, 838 and references listed therein. Also see ref 2b. (b) Constable, E. C.; Ward, M. D.; Tocher, D. A. *J. Am. Chem. Soc.* **1990**, *112*, 1256. Constable, E. C.; Ward, M. D.; Tocher, D. A. *J. Chem. Soc., Dalton Trans.* **1991**, 1675.

(5) For example, for reviews see: (a) Chidsey, C. E. D.; Murray, R. W. *Science* **1986**, *231*, 25. Wrighton, M. S. *Science* **1986**, *231*, 32. (b) Arana, C.; Yan, S.; Keshavarz-K, M.; Potts, K. T.; Abruña, H. D. *Inorg. Chem.* **1992**, *31*, 3680 and references listed therein.

(6) *Frontiers in Supramolecular Organic Chemistry and Photochemistry*; Schneider, H.-J., Dürr, H., Eds.; VCH: Weinheim, Germany, 1991. *Supramolecular Photochemistry*; Balzani, V., Scandola, F., Eds.; Horwood: Chichester, U.K., 1991.

(7) For example, see: (a) Merz, A. *Top. Curr. Chem.* **1990**, *152*, 49 and references therein. (b) Potts, K. T.; Usifer, D. A.; Guadalupe, A. R.; Abruña, H. D. *J. Am. Chem. Soc.* **1987**, *109*, 3961. Guadalupe, A. R.; Usifer, D. A.; Potts, K. T.; Hurrell, H. C.; Mogstad, A.-E.; Abruña, H. D. *J. Am. Chem. Soc.* **1988**, *110*, 3462. Hurrell, H. C.; Mogstad, A.-L.; Usifer, D. A.; Potts, K. T.; Abruña, H. D. *Inorg. Chem.* **1989**, *28*, 1080. Also see ref 5a.

(8) (a) Potts, K. T.; Keshavarz-K, M.; Tham, F. S.; Abruña, H. D.; Arana, C. *Inorg. Chem.*, two preceding papers in this issue. (b) Arana, C.; Abruña, H. D. *Inorg. Chem.* **1993**, *32*, 194.

(9) Gagne, R. R.; Spiro, C. L. *J. Am. Chem. Soc.* **1980**, *102*, 1443. Powers, M. J.; Myers, T. J. *J. Am. Chem. Soc.* **1980**, *102*, 1389. Creutz, C.; Taube, H. J. *J. Am. Chem. Soc.* **1969**, *91*, 3988; **1973**, *95*, 1086. Campagna, S.; Denti, G.; Serroni, S.; Ciano, M.; Balzani, V. *Inorg. Chem.* **1991**, *30*, 3728. Steel, P. J. *Coord. Chem. Rev.* **1990**, *106*, 227, ref 6.

(10) Munakata, M.; Kitagawa, S.; Asahara, A.; Masuda, H. *Bull. Chem. Soc. Jpn.* **1987**, *60*, 1927.

(11) Habiyakara, A.; Lucken, E. A. C.; Bernardinelli, G. *J. Chem. Soc., Dalton Trans.* **1992**, 2591. Lewin, A. H.; Michl, R. J. *J. Chem. Soc., Chem. Commun.* **1972**, 661.

(12) Crumbliss, A. L.; Poulos, A. T. *Inorg. Chem.* **1975**, *14*, 1529. Munakata, M.; Nishibayashi, S.; Sakamoto, H. *J. Chem. Soc., Chem. Commun.* **1980**, 219. Pflaum, R. T.; Brandt, W. W. *J. Am. Chem. Soc.* **1955**, *77*, 2019. Chandra, M.; O'Driscoll, K. F.; Rempel, G. L. *Prep. Czan. Symp. Catal.* **1979**, *6*, 44; *J. Mol. Catal.* **1980**, *8*, 339.

(13) (a) Foplgado, J.-V.; Henke, W.; Allmann, R.; Stratemeier, H.; Beltram-Porter, D.; Rojo, T.; Reinen, D. *Inorg. Chem.* **1990**, *29*, 2035. (b) Hogg, R.; Wilkins, R. G. *J. Chem. Soc.* **1962**, 341. (c) For a review of terpyridine coordination see: Constable, E. C. *Adv. Inorg. Radiochem.* **1986**, *30*, 69.

(14) Potts, K. T.; Cipullo, M. J.; Ralli, P.; Theodoridis, G. *J. Org. Chem.* **1982**, *47*, 3027.

0020-1669/93/1332-4450$04.00/0

Table I. Chemical Shifts (500 MHz, ppm) of Protons in the Ligands **3b,c** and in Their Bimetallic, Double-Stranded Helicates **4b,c**

proton	ligand **3b** ($CDCl_3$)	ligand **3c** ($CDCl_3$)	complex **4c** [$(CD_3)_2CO$]	complex **4c** (CD_3CN)	complex **4c** (CD_3NO_2)	complex **4b** (CD_3NO_2)
H_3[a]	8.43 (d)	8.46 (d)	7.87 (d)	7.47 (bs)	7.64 (bs)	7.66 (bs)
H_5[b]	7.59 (d)	7.61 (d)	7.60 (d)	7.20 (bs)	7.48 (bs)	7.48 (bs)
$H_{3'}$	8.67 (d)	8.67 (d)	8.04 (m)	7.81 (d)	7.81 (d)	7.82 (d)
$H_{4'}$	7.99 (t)	7.98 (t)	8.04 (m)	7.88 (t)	7.95 (t)	7.97 (t)
α	8.15 (d)	8.13 (d)	7.66 (m)	7.64 (d)	7.65 (d)	7.69 (d)
β	7.52 (t)	7.52 (t)	7.16–7.11 (m)	6.96 (bt)	7.10 (bt)	7.12 (bt)
γ	7.45 (bt)	7.45 (bt)	7.16–7.11 (m)	7.09 (bt)	7.15 (bt)	7.17 (bt)
$-S-CH_2-$		3.17 (t)	3.38 (m)	2.93 (m)	3.29 (m)	
$-CH_2-$		1.89 (sext)	1.92 (m)	1.68 (m)	1.93 (m)	
$-CH_3$		1.17 (t)	1.18 (t)	1.04 (t)	1.19 (t)	
$-S-CH_3$	2.67 (s)					2.79 (s)

[a] H_3/H_5. [b] H_5/H_3 for complexes **4b** and **4c**.

mixture was stirred at room temperature for 24 h when glacial acetic acid (35 mL) and ammonium acetate (6.2 g, 8.04 × 10^{-2} mol) were added, followed by refluxing the mixture for 2 h with continuous distillation of THF from the mixture. After cooling of the reaction mixture to room temperature, it was poured onto ice (60 g) and diluted with cold water (20 mL) and set aside for 3 h. The separated orange-colored solid was collected, washed with cold water, and dried: 1.3 g. Recrystallization from chloroform (activated charcoal) afforded the ligand **3b** as colorless prisms: 1.1 g (53%); mp 210–212 °C; ^{1}H NMR data (500 MHz, $CDCl_3$) δ 8.67 (d, 2, $H_{3'}$, $H_{5'}$, $J_{4',3'}$ = 7.6 Hz), 8.43 (bs, 2, H_3, $H_{3''}$), 8.15 (bd, 4, H_α, H_α, $H_{\alpha'}$,$J_{\beta,\alpha}$ = 7.7 Hz), 7.99 (t, 1, $H_{4'}$, $J_{3',4'}$ = 7.6 Hz), 7.59 (bs, 2, H_5, $H_{5''}$), 7.52 (t, 4, H_β, $H_{\beta'}$, $J_{\alpha,\beta}$ = 7.7 Hz), 7.45 (t, 2, H_γ, $H_{\gamma'}$, $J_{\beta,\gamma}$ = 7.5 Hz), 2.67 (s, 6, SCH_3); mass spectrum (EI) *m/z* (% relative intensity) 477 (100) [M^+]. Anal. Calcd for $C_{29}H_{23}N_3S_2$: C, 72.94; H, 4.86; N, 8.80. Found: C, 72.78; H, 4.77; N, 8.60.

The corresponding 6,6″-diphenyl-4,4″-bis(*n*-propylthio)-2,2′:6′,2″-terpyridine (**3c**) was prepared in a similar way from acetophenone (1.04 g, 8.6 × 10^{-3} mol) and 2,6-bis[3,3-bis(*n*-propylthio)-1-oxo-2-propen-1-yl]pyridine[14] (**1b**) (2.10 g, 4.3 × 10^{-3} mol), the yield of crude ligand being 1.5 g. It crystallized from cyclohexane (activated charcoal) as colorless prisms: 1.1 g (48%); mp 142–145 °C; ^{1}H NMR data in Table I mass spectrum (EI) *m/z* (% relative intensity) 534 (17) [M^+]. Anal. Calcd for $C_{33}H_{31}N_3S_2 \cdot H_2O$: C, 73.48; H, 5.85; N 7.79. Found: C, 73.77; H, 5.77; N, 7.75.

Doubled-Stranded Helicate 4c Formation from Ligand 3c. The ligand **3c** (100 mg, 1.87 × 10^{-4} mol) was added to a colorless methanolic solution (10 mL) of [$Cu^I(CH_3CN)_4$][PF_6] (70 mg, 1.87 × 10^{-4} mol) at ambient temperature. An immediate color change to a dark-red solution marked the complexation. After the reaction mixture was stirred at room temperature for 3 h, the separated red salt was collected and then washed with methanol followed by anhydrous diethyl ether: 140 mg (100%). Recrystallization of this red powder from nitromethane:diethyl ether afforded the complex **4c** as dark-red prisms: mp 294–296 °C; λ_{max} 550 nm [$\epsilon = 1.87 \times 10^3$ (cm M)$^{-1}$]; mass spectrum (FAB) *m/z* 1213.5 [$L_2M_2F^+$], 1129.5 [L_2M^+], 596.4 [LM^+]. Anal. Calcd for $C_{66}H_{62}Cu_2F_{12}N_6P_2S_4 \cdot H_2O$: C, 52.76; H, 4.29; N, 5.59. Found: C, 52.49; H, 4.05; N, 5.60.

Reaction of the ligand **3b** with [$Cu^I(CH_3CN)_4$][PF_6] following the above procedure gave the complex **4b** as dark-red prisms in 91% yield: mp 318–320 °C; ^{1}H NMR data (500 MHz, CD_3NO_2) δ 7.97 (t, 2, $H_{4'}$, $J_{3',4'}$ = 7.9 Hz), 7.83 (d, 4, $H_{3'}$, $H_{5'}$, $J_{4',3'}$ = 7.9 Hz), 7.69 (d, 8, H_α, $H_{\alpha'}$, $J_{\beta,\alpha}$ = 7.6 Hz), 7.66 (d, 4, $H_{3/5}$, $H_{3''/5''}$, $J_{5,3}$ = 1.5 Hz), 7.48 (d, 4, $H_{3/5}$, $H_{3''/5'}$, $J_{5,3}$ = 1.5 Hz), 7.17 (bt, 4, H_γ, $H_{\gamma'}$, $J_{\beta,\gamma}$ = 7.3 Hz), 7.12 (bt, 8, H_β, $H_{\beta'}$, $J_{\gamma,\beta}$ = 7.3 Hz), 2.79 (s, 12, SCH_3); mass spectrum (FAB) *m/z* 1227.1 [$L_2M_2 \cdot PF_6^+$, 1082.2 [$L_2M_2^+$], 1018 [L_2M^+]. Anal. Calcd for $C_{58}H_{46}Cu_2F_{12}N_6P_2S_4$: C, 50.77; H, 3.38; N, 6.12. Found: C, 50.68; H, 3.26; N, 6.03.

In a similar fashion the ligand **3a** (200 mg, 7.1 × 10^{-4} mol) and [$Cu^I(CH_3CN)_4$][PF_6] (265 mg, 7.1 × 10^{-4} mol) gave complex **4a** as an orange powder: 155 mg (86%), mp 318–320 °C; mass spectrum (FAB) *m/z* 829.0 [$L_2M_2PF_6^+$], 686.0 [$L_2M_2^+$], 341.9 [LM^+]. Anal. Calcd for $C_{32}H_{26}Cu_2F_{12}N_6P_2S_2 \cdot 2H_2O$: C, 37.98; H, 2.98; N, 8.31. Found: C, 38.15; H, 2.51; N, 8.19.

Cu(II) Complex 5 Derived from Ligand 3a. The ligand **3a** (28.2 mg, 1.0 × 10^{-3} mol) was added to a solution of $Cu(OAc)_2 \cdot H_2O$ in methanol (20 mL) at ambient temperature. The reaction mixture was stirred at room temperature for 3 h, and a saturated methanolic solution of NH_4PF_6 (400 mg) was then added. The resultant green precipitate was collected and washed with water, followed by methanol and diethyl ether. Recrystallization from acetonitrile:diethyl ether resulted in 432 mg (95%) of bluish-green prisms of **5**: mp > 300 °C; λ_{max} 698 nm; mass spectrum (FAB) *m/z* 310 [L_2M^{2+}]. Anal. Calcd for $C_{32}H_{26}CuF_{12}N_6P_2S_2$: C, 42.10; H, 2.85; N, 9.21. Found: C, 41.94; H, 2.64; N, 9.14.

X-ray Structural Determination. Crystal selection and mounting were done in a cold room (2 °C) to reduce the rate of loss of nitromethane of crystallization and subsequent deterioration of the crystal. A selected crystal was immediately immersed in epoxy resin, and the crystal was then attached onto a glass fiber before the epoxy hardened. After the epoxy had set for 1 h, the crystal was mounted on a goniometer head, and Siemens standard procedures and programs were used for all operations.

Crystal Data for Complex 4b: $C_{58}H_{46}Cu_2N_6S_4 \cdot 2(CH_3NO_2$, orthorhombic dark-red prism of 0.22 × 0.50 × 0.72 mm, $M = 1494.4$, space group *Pbcn* (No. 60), $a = 16.060(4)$ Å, $b = 15.023(5)$ Å, $c = 26.751(7)$ Å, $\alpha = \beta = \gamma = 90°$, $V = 6454(3)$ Å^3, $Z = 4$, $D_c = 1.536$ Mg m^{-3}. Data were collected at room temperature (21 °C) using a Siemens R3m diffractometer with Mo Kα radiation (graphite monochromator; λ = 0.710 69 Å) in a Wyckoff scan mode (ω range = 1.20° +[$2\theta(K\alpha_1)-2\theta(K\alpha_2)$]; 2θ range = 3–48°). The reflections were measured with a variable scan speed (2.50–29.30°/min) and an ω scan range of 1.20°, four check reflections being measured for every 60 reflections in a total of 5644 reflections of which 3036 were uniquely observed ($F > 4.0\sigma(F)$). Lorentz, polarization, and semi-empirical absorption corrections were applied [μ(Mo) = 0.92 mm^{-1}; maximum and minimum transmission factors were 0.379 and 0.327, respectively]. Siemens programs, SHELXTL PLUS (release 4.21/V), were used for phase determination and structure refinement. The distribution of intensities ($E^2 - 1 = 1.067$) and systematically absent reflections indicated a centrosymmetric space group, *Pbcn* (No. 60), and the data were refined using this space group. The positions of the two copper atoms were identified in a Patterson vector map. These two copper atoms were located on a 2-fold rotation axis, parallel to the *b*-axis. Direct methods of phase determination led to an electron-density map from which the non-hydrogen atoms were identified, except the molecule of nitromethane of crystallization. Subsequent isotropic refinement led to the identification of the molecule of nitromethane in the asymmetric unit. Atomic coordinates and isotropic and anisotropic temperature factors of all non-hydrogen atoms were refined by means of full-matrix least-squares procedures. All hydrogen atoms were included in the refinement in calculated positions riding on the atoms to which they were attached and with fixed isotropic temperature factors. The refinement converged at $R = 6.68\%$ and $R_w = 9.04\%$, and the background in the electron-density map was 1.32 e/Å^3.

Discussion

(a) Ligand Synthesis. Terpyridine derivatives along with other oligopyridines have been synthesized by metal coupling reactions[15] or by cyclocondensation of 1,5-diones[16] or 1,5-enediones[14] with ammonia or other nitrogen source. Nucleophilic aromatic

---

(15) Newkome, G. R.; Pantaleo, D. C.; Puckett, W. E.; Ziefle, P. L.; Deutsch, W. A. *J. Inorg. Nucl. Chem.* **1981**, *43*, 1529. Rode, T.; Breitmaier, E. *Synthesis* **1987**, 575. Tecco, M.; Testaferri, L.; Tingoli, M.; Chianelli, D.; Montanucci, M. S. *Synthesis* **1984**, 736. Parks, J. E.; Wagner, B. E.; Holm, R. H. *J. Organomet. Chem.* **1973**, *56*, 53.

(16) Gill, N. S.; James, K. B.; Lions, F.; Potts, K. T. *J. Am. Chem. Soc.* **1952**, *74*, 4923.

Scheme I. Synthesis and Complexation of Substituted 2,2′:6′,2″-Terpyridines (**3**)

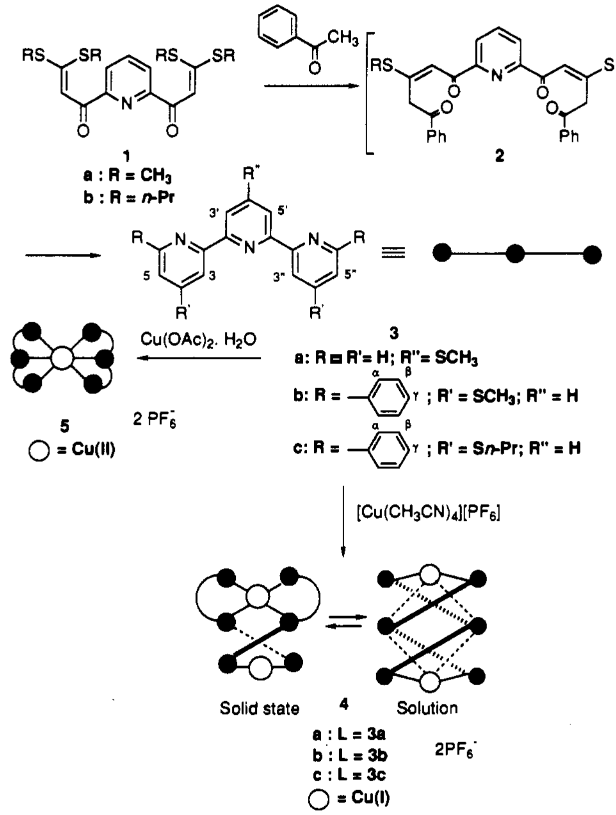

substitution of terpyridine with alkyl- or phenyllithiums[17a] provides for introduction of substituents into the 6,6″-positions. The enedione approach is by far the most useful due to its wide scope for substituent introduction. Routes to the intermediate 1,5-diones stem from a common principle and are variations of the Kröhnke procedure,[18] which allows the introduction of aromatic substituents in the terpyridine structure. The Mannich base approach has been utilized to prepare other important intermediates in this area,[19] while terpyridines functionalized in the 4′-pyridine position[7a,20] are now readily accessible by the α-oxoketene dithioacetal method.[14] The synthesis of 6,6″-diphenyl-4,4″-bis(alkylthio)-2,2′:6′,2″-terpyridines **3b,c** using the α-oxoketene dithioacetal method is shown in Scheme I, the other 4′-substituted terpyridines **3a** having been prepared earlier by this general procedure.[14]

(b) Complex Formation and Characterization. Reaction of 4′-(methylthio)-2,2′:6′,2″-terpyridine (**3a**) and tetrakis(acetonitrile)copper(I) hexafluorophosphate[21] in dry, deoxygenated methanol at room temperature gave an immediate orange-red product **4a** of composition $[L_2M_2]^{2+}$. This molecular formula was established from combustion analytical and FAB mass spectral data[22] {*m/z* 829.5 $[M^+ - PF_6]$}. Although stable in the solid state, in solution (CH_3CN, CH_3NO_2, DMF, acetone, DMSO, etc.) it underwent oxidative rearrangement to form the octahedral cupric complex **5** with λ_{max} 698 nm, and this complex was also synthesized from ligand **3a** and $Cu(OAc)_2$. This absorption maximum should be compared with λ_{max} 680 nm reported[13b] for $[(terpy)_2Cu]^{2+}$.

Reaction of 6,6″-diphenyl-4,4″-bis(methylthio)-2,2′:6′,2″-terpyridine (**3b**) with the Cu(I) source under the above reaction conditions resulted in an orange-red product **4b**, $[L_2M_2]^{2+}$, which crystallized as dark-red prisms from nitromethane with the slow diffusion of diethyl ether. Analytical and FAB mass spectral data[22] {*m/z* 1227.1 $[M^+ - PF_6]$, 1082.2 $[M^+ - 2PF_6]$} allowed the assignment of this molecular formula. An absorption band at 550 nm [$\epsilon = 1.87 \times 10^3$ (cm M)$^{-1}$] attributable to an MLCT transition is characteristic of oligopyridine–Cu(I) complexes.[3b,4a,8a] The X-ray structure of **4b** is shown in Figure 1. The two ligand strands are intertwined about each other and around the Cu(I) ions in a double-helical fashion, the result of a series of twists about the interannular C–C bonds in each ligand strand. The interannular angles between rings A and B, B and C, C and D, and D and E are 34.1, 27.5, 37.0, and 45.6°, respectively. A unique feature of the structure is the distorted tetrahedral and linear coordination geometries of the Cu(I) ions. The significant differences in the distances between the two middle pyridine rings' nitrogen atoms and the Cu(I) centers [N(3)–Cu(1) = 2.180(5) Å; N(3)–Cu(2) = 2.480(5) Å] and the N–Cu–N bond angles [N(3)–Cu(1)–N(3a) = 122.4(3)°; N(4)–Cu(2)–N(4a) = 176.0(3)°] clearly demonstrate the difference in each metal's solid-state environment. The two Cu(I) ions are located along the 2-fold rotation axis parallel to the *b*-axis of the unit cell. Due to this unique symmetry position the first strand of the ligand will generate the second strand by this 2-fold rotation symmetry operation and, as a result, both strands of the ligand will have identical structural parameters.

The helix is flat with a pitch height of 8 Å, and the Cu–Cu distance (bond?)[28] is 2.631(2) Å. The diameter of the circumscribed cylinder measured from C24 to C24A is 9.437 Å and that measured from C44 to C44A is 9.37 Å. The π–π interaction between all aromatic rings in the assembly (Figure 1B,C) produced four sets of stacks. Two sets of triple stacks resulted from the middle pyridine rings being "sandwiched" between the two terminal phenyl rings of the other strand with an average distance of 3.80 Å. Two additional sets of double stacks resulting from the other two pyridine rings of each strand were also present with an average distance of 3.55 Å.

^{1}H NMR Characterization of Complex 4. The ^{1}H NMR spectra (Figures 2 and 3) of the ligand **3c** and its complex **4c** are especially informative and provide an insight into the stability of the complex in solution, its solution structure, and its chiral nature. The NMR spectrum of the complex which was precipitated from the reaction mixture establishes that the self-assembly process results in the formation of one product only. The chemical shifts (Table I) of the protons in the complex occurred upfield to those of the free ligand with a significant change in the overall pattern of the chemical shifts. Similar changes have been observed[3b,8a] previously for the protons in Cu(I) double-stranded helical complexes derived from alkylthio-substituted oligopyridines. These observed upfield shifts are most likely due to the helical nature of the complex in which the aromatic protons are positioned in the shielding zone of the neighboring aromatic rings. These changes in chemical shifts are in contrast to those observed for the corresponding protons in the simple tetrahedral bipyridine–CU(I) complex[17b] $[L_2M]^+$ in which the overall trend is a downfield shift except for H_3. This proton's upfield shift is due to a ligand

---

(17) (a) Dietrich-Buchecker, C. O.; Marnot, P. A.; Sauvage, J. P. *Tetrahedron Lett.* **1982**, 5291. (b) Dietrich-Buchecker, C. O.; Marnot, P. A.; Sauvage, J. P. *Nouv. J. Chim.* **1984**, *8*, 573.

(18) Kröhnke, F. *Synthesis* **1976**, 1.

(19) Newkome, G. R.; Hager, D. C.; Kiefer, G. E. *J. Org. Chem.* **1986**, *51*, 850. Hedge, V.; Jahng, Y.; Thummel, R. P. *Tetrahedron Lett.* **1987**, 4023.

(20) Cuenoud, B.; Shepartz, A. *Tetrahedron Lett.* **1991**, 3325. Suavage, J. P.; Ward, M. *Inorg. Chem.* **1991**, *30*, 3869.

(21) Kubas, G. J. *Inorg. Syn.* **1979**, *14*, 90.

(22) 3-Nitrobenzyl alcohol was used as the matrix in these FAB mass spectra, determined on a ZAB mass spectrometer, at the University of Illinois.

(23) Abel, E. W.; Long, N. J.; Orrell, K. G.; Osborne, A. G.; Pain, H. M.; Silk, V. *J. Chem. Soc., Chem. Commun.* **1992**, 303.

(24) Alemany, P.; Alvarez, S. *Inorg. Chem.* **1992**, *31*, 4265.

(25) Potts, K. T.; Fessak, A. Unpublished results.

(26) Jennings, W. B. *Chem. Rev.* **1975**, *75*, 307.

(27) Piguet, C.; Bernardinelli, G.; Williams, A. F. *Inorg. Chem.* **1989**, *28*, 2920. Ruttimann, S.; Piguet, C.; Bernardinelli, G.; Bocquet, B.; Williams, A. F. *J. Am. Chem. Soc.* **1992**, *114*, 4230.

(28) Cotton, F. A.; Feng, X.; Matusz, M.; Poli, R. *J. Am. Chem. Soc.* **1988**, *110*, 7077.

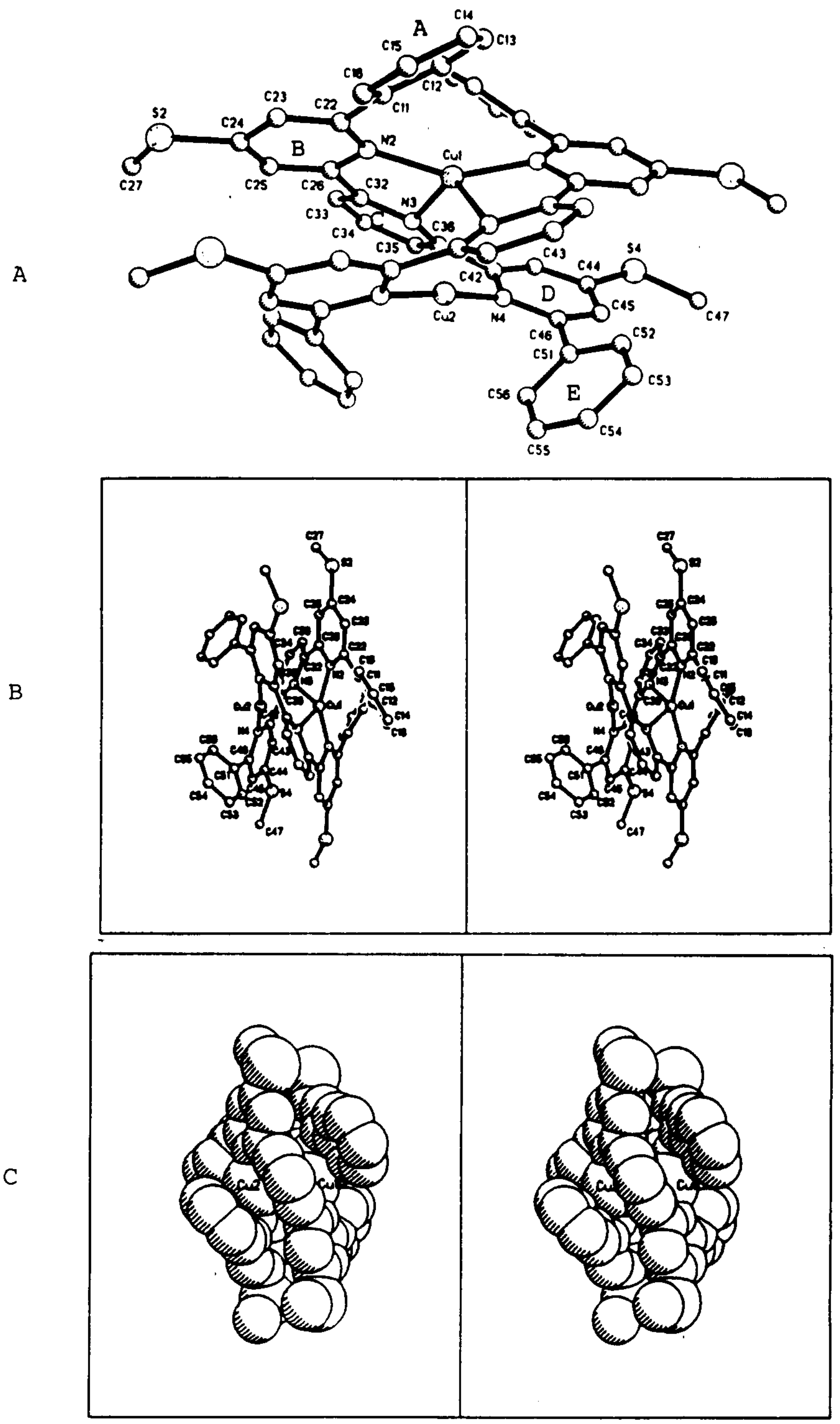

Figure 1. A. X-ray structure of the right-handed (P) double-stranded helical complex **4b**. Selected distances (Å): Cu(1)–Cu(2) = 2.63(2), Cu(1)–N(2) = 1.978(5), Cu(2)–N(4) = 1.926(5). Bond angles (deg): N(2)–Cu(1)–N(2a) = 152.2(3), N(3)–Cu(1)–N(3a) = 122.4(3), N(2)–Cu(1)–N(3) = 81.9(2), N(4)–Cu(2)–N(4a) = 176.0(3). B. Stereotopic view of **4b**. C. Stereotopic space-filling representation of **4b**.

conformational change from transoid to cisoid upon complexation with Cu(I) ions.

The ^1H NMR spectra of the complex **4c** determined in different solvents (Figure 2) clearly showed the solvent dependency of the chemical shifts of the aromatic protons as well as the protons of the *S*-*n*-propyl groups. The aromatic protons in the spectrum of complex **4c** determined in CD_3CN, a relatively strong coordinating solvent for Cu(I) salts, are as well resolved as the protons in its spectrum determined in CD_3NO_2, a weak coordinating solvent. This establishes the unusual stability of the diphenylterpy–Cu(I) complex in acetonitrile solution, which is in contrast to the general instability of terpyridine–Cu(I) complexes in solution.[12] Although the patterns of the chemical shifts of the diphenylterpy–Cu(I) complex in these two solvents are very similar, the solvent dependencies of H_3 and H_5 are distinctive, as demonstrated in Figure 2C,D. In acetone solution (Figure 2B) the same number of chemical shifts are observed, and it is interesting to note that $H_{3'}$ and $H_{4'}$ are isochronous in this solvent.

Symmetry elements in the ligand **3c** reduced the observable number of protons to seven (out of a total of seventeen aromatic protons), the same number of protons that were observed in the complex **4c** where there is a total of 34 aromatic protons in both strands. The number of protons suggests that, in solution, the complex **4c** has an additional C_2 symmetry axis present which bisects the two middle pyridine rings and which is perpendicular to the Cu–Cu axis, this additional symmetry being absent in the

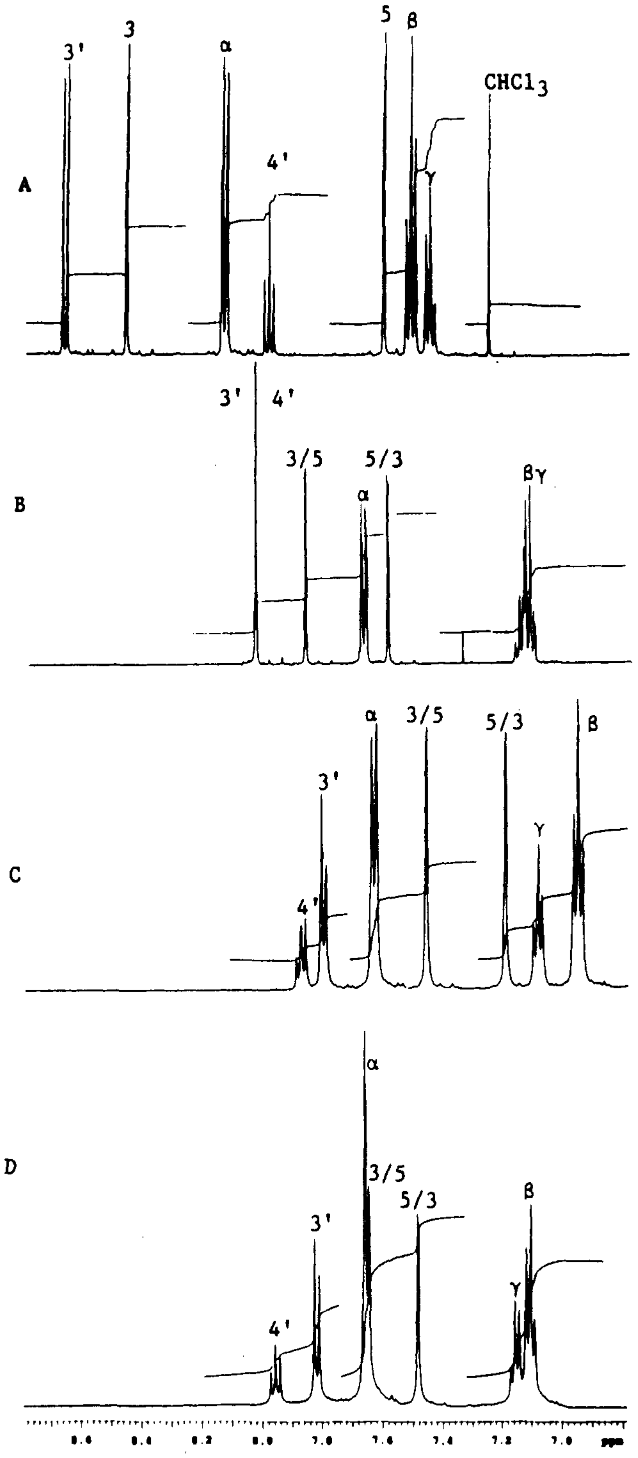

Figure 2. ^{1}H NMR spectra (500 MHz) of the aromatic regions of (A) the ligand **3c** ($CDCl_3$) and the complex **4c** (B) in $(CD_3)_2CO$, (C) in CD_3CN, and (D) in CD_3NO_2.

solid state. This overall symmetry in the complex may be accommodated in essentially three ways. The first possibility involves a fluxional-type mechanism where the two middle pyridine rings oscillate between the two cationic binding centers faster than the NMR time scale at room temperature. To evaluate this possibility, the NMR spectrum of complex **4b** was determined in deuterated acetone at −80 °C and also in deuterated acetonitrile at −40 °C, these temperatures being the lower limits for the solvents. No significant chemical shift changes were observed in either the aromatic or aliphatic region of either spectrum compared to room-temperature spectra. If the fluxional change were slowed at low temperatures, one would anticipate that the additional C_2 axis of symmetry would no longer be present, resulting in a symmetry similar to that present in the solid-state structure. This change would be reflected in a greater number of nonequivalent aromatic protons in each ligand strand and the two sets of alkyl protons. In the preceding paper[8a] we have also shown that when such a C_2 symmetry axis is absent in a double-stranded helicate, all the protons in the ligand strand become nonequivalent.

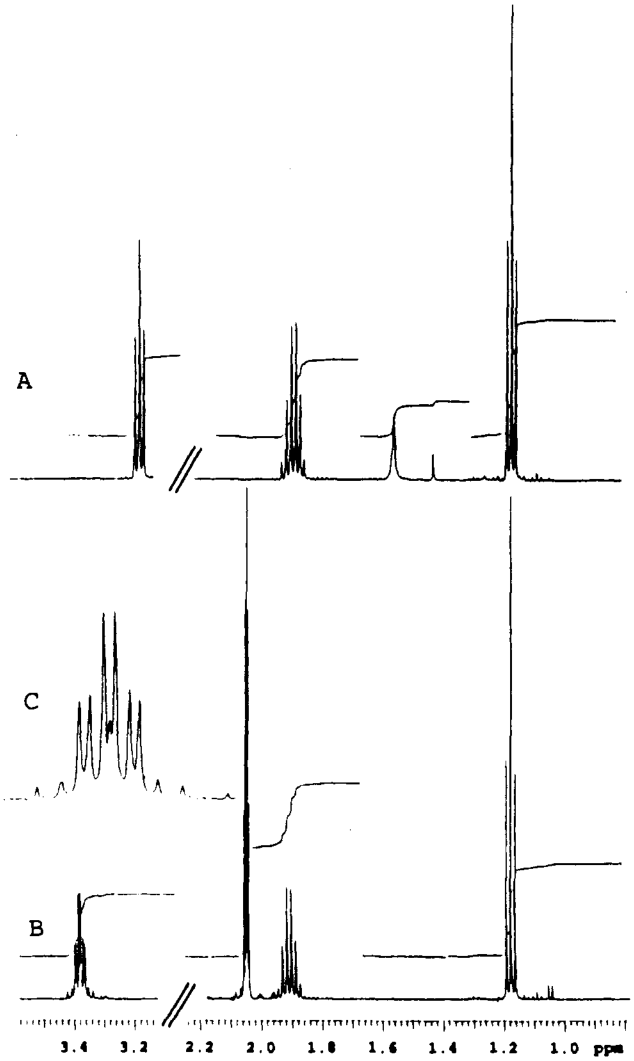

Figure 3. ^{1}H NMR spectra (500 MHz) of the aliphatic region of (A) the ligand **3c** ($CDCl_3$), (B) the complex **4c** in $(CD_3)_2CO$, and (C) the expanded multiplet of the *S–CH₂–* protons of **4c** at δ 3.39.

The behavior of complex **4c** described above should be contrasted with that of the monometallic rhenium bromo tricarbonyl complex of terpyridine and related compounds.[23] In this complex terpyridine acts as a bidentate ligand with one uncoordinated pyridine ring at room temperature. At elevated temperatures (140 °C for the rhenium complex), these complexes undergo a fluxional change with the metal ion oscillating between both terminal pyridine rings.

A second possibility is of particular interest and calls for the two sets of lone pair electrons from the two middle pyridine rings to be coordinated to both Cu(I) ions, generating a diamond-like tetrahedral geometry. These types of electron-deficient diamond structures have been the subject of recent theoretical studies[24] by Alvarez to determine the correct description of the binding and the strength of the metal–metal bond on the basis of orbital topology and framework electron count procedures. Figure 4 shows the bond distances of **4b** in the solid state. These data demonstrate that only a small conformational change in solution is needed for the nitrogen lone pair electrons of the two middle pyridine rings to become accessible to either metal with generation of the symmetrical diamond structure. The short Cu–Cu distance of 2.631(2) Å determined experimentally in complex **4b** is in

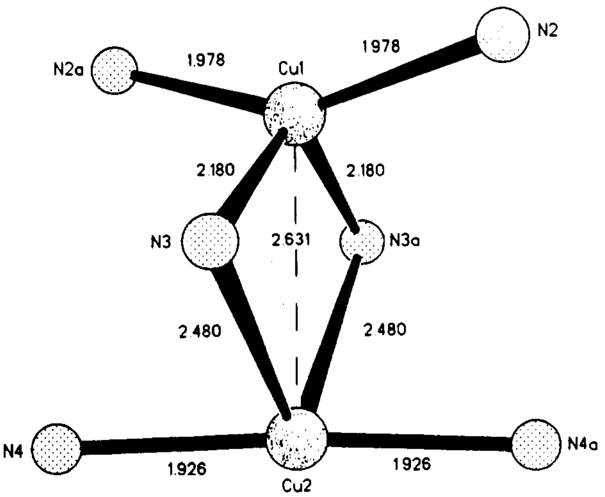

Figure 4. Cu and N bond distances (Å) in complex **4b** in the solid state.

Table II. Formal Potentials[a] of Complex **4b** in Different Solvents

solvent	$E^{\circ\prime}(1)$ (ΔE_p)	$E^{\circ\prime}(1)$ (ΔE_p)
acetonitrile	+0.12 (80)	+0.98 (130)
nitromethane	+0.09 (120)	+0.75 (100)
methylene chloride	+0.47 (160)	+0.80 (140)

[a] V vs SSCE.

general agreement with Alvarez's discussion of his more symmetrical structures, and complex **4b** provides a unique example of this type of compound for further studies. Representation of **4b** in this manner would be consistent with the more symmetrical geometry observed in solution.

A third possibility is that the two middle pyridine rings act as an intersite bridge. In this situation their two sets of lone pair electrons are not coordinated to either Cu(I) ion, resulting in both Cu(I) ions having linear-like coordination geometry. Even though we cannot preclude this possibility on the basis of the available NMR data, such a structure would be most unlikely in a double-stranded helicate of this size. The pitch of the helix is very small (pitch height 8 Å, including phenyl substituents) causing each pyridine's lone pair of electrons to be in close proximity to each other. Such a spatial relationship could possibly result in a Coulombic repulsion between the pyridine nitrogen's lone pairs of electrons. In addition the unusual metal–metal interaction observed by electrochemical analysis ($\Delta E^{\circ\prime}$ = 860 mV; see below) could be the result of these two pyridine rings mediating the communication between the two electroactive centers. In other work, we have recently prepared[25] analogous new Cu(I)-containing helical complexes where the middle pyridine ring was replaced by an alkyl or alkenyl intersite bridge. These complexes have very different coordination geometries and electrochemical properties. The significant differences between the coordination behavior of these new types of ligands and the diphenyl-substituted terpyridines suggest very strongly that the middle pyridine rings play a key role in determining the geometry, stoichiometry, and physical properties of the resultant complex.

We have shown in a preceding publication[8a] that *S*-alkyl groups introduced into the pyridine 4-position during ligand synthesis to enhance functional group interconversions and solubility may be utilized in the ^{1}H NMR characterization of the derived complexes. The –S–CH$_2$–R (R ≠ H) group can serve as an ^{1}H NMR probe for determining the chirality of a molecule.[26] We have utilized this characteristic property to establish the solution stability and helical chirality of complex **4c** which contains an S–CH$_2$–CH$_2$–CH$_3$ substituent at the 4-position of the terminal pyridine rings of the terpyridine unit. The enantiotopic –CH$_2$– group has an A$_2$ spin system (triplet) in an achiral molecule, in this case the ligand (Figure 3A), whereas when the –CH$_2$– group is situated in a chiral environment (the helix), its spin system changes to an AB type (multiplet) (Figure 3B,C). One should note that this type of geminal coupling ($\Delta\delta$) can be affected by several factors. In general, the couplings of these protons depend significantly on temperature and solvent as well as structure.[26] In the case of the complex **4c** the second –CH$_2$– group in the *S*-*n*-propyl group is, in principle, a diastereotopic center. However, the magnitude of $\Delta\delta$ in complex **4c** is considerably depressed as the distance between the –CH$_2$– group and the asymmetric helical structure is appreciably greater than with the –CH$_2$– group adjacent to the sulfur atom. The $\Delta\delta$ of both –CH$_2$– groups is solvent dependent, and the sulfur's two lone pairs of electrons may also influence the solvent effect. The degree of AB coupling in complex **4c** is more pronounced in solvents with lower dielectric constant, e.g., acetone (ϵ = 22), and less pronounced in solvents with higher dielectric constants, e.g., nitromethane (ϵ = 34) and acetonitrile (ϵ = 36). It is interesting to contrast the results described above, especially the stability of the complex **4c** with those reported[27] recently for the 2,6-bis(benzimidazol-2-yl)pyridine–Cu(I) complex.

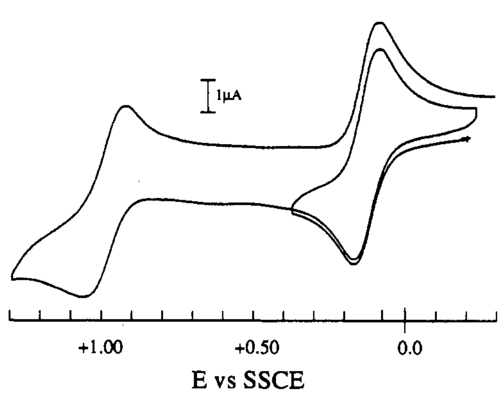

Figure 5. Cyclic voltammogram at a platinum electrode and at 100 mV/s for a 1.1 mM solution of complex **4b** in acetonitrile/0.1 M TBAP.

Electrochemical Characterization of Complex 4b. The electrochemical behavior of complex **4b** is unusual in a number of respects, and before discussing this behavior, it is informative to briefly describe the electrochemical behavior of the closely related complex [Cu^{II}(mt-terpy)$_2$]$^{2+}$ (**5**) (mt = methylthio). In acetonitrile solution this complex underwent a reversible one-electron reduction at –0.29 V (vs SSCE) which corresponded formally to a Cu(II/I) process. There was an additional reduction at a peak potential value of ca. –0.62 V which corresponded to further reduction and deposition of metallic copper, indicated by the appearance of a stripping peak whose amplitude grew as a function of time at a potential at or beyond –0.62 V. In contrast, complex **4b** exhibited two oxidative waves whose potentials and degree of reversibility were a strong function of solvent (Table II). In acetonitrile (Figure 5) the oxidation waves were at $E^{\circ\prime}$ values +0.12 (ΔE_p = 80 mV) and +0.98 (ΔE_p = 130 mV) V *vs* SSCE, respectively, with the latter showing some kinetic limitations.

An initial comparison may be made between the behavior of complex **4b** and that of [Cu^{II}(mt-terpy)$_2$]$^{2+}$ (**5**) in acetonitrile. The fact that in the former the potential was shifted positively by about 400 mV would suggest that the diphenylterpy ligand stabilized copper in the +1 oxidation state much more strongly than does mt-terpy itself. However, since acetonitrile is a moderately strong coordinating solvent and since the [Cu(I)(CH$_3$CN)$_4$]$^+$ complex oxidizes at about +0.93 V, these waves could imply that in acetonitrile the complex was decomposing to give a monomeric copper complex as well as the acetonitrile complex. The observation of an oxidation at +0.12 V argues against such a process being operative. It should also be noted that the dimeric complex **4a** without phenyl substituents, although stable in the solid state, decomposed in solution to yield the monomeric copper(II) complex and the acetonitrile complex, shown by spectrophotometric and electrochemical measurements. Supporting evidence for the retention of the double-stranded helicate structure comes from the fact that in nitromethane, a very weak coordinating solvent with a dielectric constant similar to that of acetonitrile, two waves were also obtained, albeit at potentials shifted somewhat negatively when compared to those observed in acetonitrile. Oxidation of the sulfur in the *S*-alkyl side chains can be ruled out since the electrochemistry of these free ligands and related alkylthio-substituted oligopyridines resulted in totally irreversible and multielectron oxidation processes.

Solution studies (vide supra) suggest that the bimetallic complexes are highly symmetrical and that the two Cu(I) centers are chemically equivalent. The difference in metal-based oxidation potentials in symmetrical homobimetallic complexes has been used[9] as a measure of the degree of metal–metal interaction. Assuming (as our data suggest) that the two copper centers are equivalent in solution, then the large value of $\Delta E^{\circ\prime}$ = 860 mV would be indicative of a high degree of metal–metal interaction possibly mediated/modulated by the ligand. This value of $\Delta E^{\circ\prime}$ is the largest that we have observed in our studies to date and should be compared with that obtained, $\Delta E^{\circ\prime}$ = 503 and 496 mV, with the trimetallic Cu(I) complex prepared[8a] from a substituted quinquepyridine ligand which had a similar coordination geometry about the Cu(I) centers.

Conclusions

Ligand modification by the introduction of aryl substituents at strategic positions in the ligand has, in the case of terpyridine, enabled the stabilization of Cu(I) double-stranded helical complexes, both in the solid state and in solution. The bimetallic helical complex **4c** represents the first stable double-stranded helicate obtained from a terpyridine ligand and Cu(I), and it is also the first reported oligopyridine complex that contains two Cu(I) cations with different coordination numbers in the solid state and which, in solution, adopts a more symmetrical geometry. This behavior is most likely assisted by the small pitch of the helix which results in a short distance between the two Cu(I) atoms [2.631(2) Å], thus making the nitrogen lone pair electrons of the two middle pyridine rings accessible to either metal. A representation in terms of a diamond structure is an interesting structural possibility.

By the use of a "built-in" ^{1}H NMR probe and high-field NMR data we have been able to show both the solution stability and chiral nature of the diphenylterpy–Cu(I) double-stranded helical complex. This stability in solution was also reflected in the significant degree of metal–metal interaction observed electrochemically, with an extremely large difference in formal potentials ($\Delta E^{\circ\prime}$ = 860 mV) being present between the two one-electron oxidations. Extensive π–π stacking (four sets, 3.5–3.8 Å) is thought to be partially responsible for the observed solution stability of the molecule.

The formation of the complex **4c** is an interesting example of molecular recognition and cooperative binding. It emphasizes how, when ligands are designed to favor certain interactions as well as to take advantage of favorable solubility in solvents at ambient temperatures, the self-assembly process leads to interesting structures in extremely high yields. These concepts of ligand modification, π–π stacking enhancement, and steric protection from the environment have appreciable potential for application to related transition metals complexes, especially those containing "uncommon" oxidation states and geometry. Additional examples of these types are currently under investigation.

Acknowledgment. We thank Dr. R. Kullnig for his interest and encouragement during the X-ray structural determination, the NSF (Grant CHE-9105906) and USPHS (Grant S-10RR06245) for funds for the purchase of the 500-MHz spectrometer and American Cyanamid Co. and the Material Science Center at Cornell University for their support of this work. We also thank Dr. R. Milberg, University of Illinois, for the mass spectral determinations.

Supplementary Material Available: Tables of atomic coordinates, bond distances, bond angles, anisotropic thermal parameters, and hydrogen atom positions for complex **4b** (8 pages). Ordering information is given on any current masthead page.